Research Square

Preprints are preliminary reports that have not undergone peer review.
They should not be considered conclusive, used to inform clinical practice,
or referenced by the media as validated information.

Potential of laser-driven VHEEs toward FLASH radiotherapy: Monte Carlo dosimetric study of single-field pencil beam scanning of a brain tumor

Leonida Antonio Gizzi
Consiglio Nazionale delle Ricerche - Istituto Nazionale di Ottica (CNR-INO)
Damiano Del Sarto
Clinica San Rossore
Federico Avella
Consiglio Nazionale delle Ricerche - Istituto Nazionale di Ottica (CNR-INO)
Gabriele Bandini
Consiglio Nazionale delle Ricerche - Istituto Nazionale di Ottica (CNR-INO)
Simona Piccinini
Consiglio Nazionale delle Ricerche - Istituto Nazionale di Ottica (CNR-INO)
Davide Terzani
Lawrence Berkeley National Laboratory
Luca Labate
luca.labate@ino.cnr.it

Consiglio Nazionale delle Ricerche - Istituto Nazionale di Ottica (CNR-INO)

Article

Keywords:

Posted Date: August 27th, 2026

DOI: https://doi.org/10.21203/rs.3.rs-10695012/v1

License: This work is licensed under a Creative Commons Attribution 4.0 International License.
Read Full License

Additional Declarations: Competing interest reported. L.A.G., G.B. and L.L. are listed as inventors on an Italian industrial patent (application number: IT 102026000000715, granted by the Italian Patent and Trademark Office), which can potentially cover a technology related to the work described in this manuscript. The remaining authors declare no competing interests.

Potential of laser-driven VHEEs toward FLASH radiotherapy: Monte Carlo dosimetric study of single-field pencil beam scanning of a brain tumor

Leonida A. Gizzi[1,*], Damiano Del Sarto[2], Federico Avella[1], Gabriele Bandini[1], Simona Piccinini[1], Davide Terzani[1,+], and Luca Labate[1,]**

[1]Intense Laser Irradiation Laboratory, Consiglio Nazionale delle Ricerche - Istituto Nazionale di Ottica (CNR-INO), Pisa, Italy
[2]now at Clinica S.Rossore, Pisa, Italy
[+]Now at Lawrence Berkeley National Laboratory, Berkeley, USA
[*]la.gizzi@ino.cnr.it
[**]luca.labate@ino.cnr.it

ABSTRACT

Radiotherapy with Very High Energy Electron (VHEE) beams is being increasingly investigated as a new modality for the treatment of deep-seated tumours, even in view of novel protocols based on the so-called FLASH effect. Laser WakeField Acceleration (LWFA) provides a high-gradient accelerator technology for VHEE electron beams potentially enabling compact and affordable accelerators. While delivery of therapeutic VHEE doses are already at reach in the laboratory as pencil beams, LWFA also inherently features ultra-high instantaneous (i.e., within the laser pulse) dose rates, and major efforts are ongoing worldwide to provide FLASH dose rates. These beams may exhibit significant energy spread, and small transverse size. In view of a rapid clinical translation of LWFA-VHEE beams it is of a paramount importance to assess the role of these properties in the dose delivery to the patient. Here we present a study carried out via start-to-end (PIC and Monte Carlo) simulations, of the main dosimetric features of a realistic laser-driven VHEE pencil beam targeted on a brain tumor. The tumor coverage is achieved by a scanning procedure; the dose pattern resulting from tessellation, i.e. the overlapping of adjacent, square-shaped beamlets, and the role of energy spread are discussed. Dose Volume Histograms are presented. The potential role of the FLASH effect is also considered via a factor accounting for healthy tissue sparing. Finally, the foreseen technological path toward the achievement of FLASH dose rates with LWFA-VHEE beams is briefly outlined.

Introduction and motivations

Radiotherapy (RT) is an essential tool for cancer treatment, with more than 60% of new cancer patients in high income countries expected to undergo a RT treatment as part of their cancer management[1]. RT relies on the possibility of inducing lethal damage to tumor cells while keeping the adverse effects probability to the surrounding healthy tissues at an acceptable level. This is made possible by the usage of advanced dose conformation techniques and relies, ultimately, on the DNA repairing mechanisms operating more efficiently in healthy rather than in cancer cells[2]. The so-called therapeutic window identifies the useful range of radiation dose for which the probability of tumor control exceeds the probability of normal tissue damage, once repairing mechanisms take place. The quest for mechanisms able to increase this window is an active research field, whose findings would enable better treatments, in particular in the case of radio-resistant tumors and/or of tumors localized near sensitive organs. In this respect, the so-called FLASH effect[3] has sparked hope for a possible breakthrough in RT (for reviews on the matter see[4–6]). It consists in a reduction of damage to healthy tissue when the radiation dose is delivered at average dose rates of the order of several tens of Gy/s or more, often referred to as Ultra High Dose Rates (UHDR), orders of magnitude higher than the rates ($\sim$ Gy/min) used in current RT protocols. Although the fundamental mechanisms underpinning the FLASH effect have yet to be clarified[7–9], the preservation of healthy tissue at ultra-high dose rates with unaffected tumor control has now been confirmed in several studies (see[10–15] and Refs. therein).

Crucial for the clinical translation of FLASH-based RT protocols are the properties of the radiation sources. Indeed, the dose rate needed for FLASH treatments requires high beam current, which is out of the range of operation of clinical accelerators used for the treatment of deep seated tumors, mainly because of the poor intrinsic conversion efficiency of the underlying *Bremsstrahlung* process leading to the generation of the deep penetrating photon beam starting from the $\sim 10-20$ MeV primary electron beam. Experiments carried out so far to investigate the FLASH effect, either *in vitro*, *in vivo* or as a compassionate

treatment of superficial tumors in humans, have been carried out using conventional devices modified to provide ultra-high dose rates (see[16,17] and Refs. therein). In the vast majority of cases, electron beams with relatively low energy have been used, only suitable for tumor irradiation at shallow depths[15], such as in the case of skin[18], eyes, salivary glands tumors[19], or in IORT[20]. Electron beams capable of delivering FLASH dose rates, for instance, have been obtained by standard medical accelerators, by removing the electron-to-photon conversion element and tuning the beam forming and accelerating structures to sustain the needed high currents, and to provide, at the same time, beams with a suitable quality[21–23]; electrons with a maximum energy up to $\sim 20\,\mathrm{MeV}$ can be obtained in this way. Moreover, electron accelerators used for Intra Operative Radiation Therapy (IORT) are also available with FLASH dose-rates, with energy up to $\sim 10\,\mathrm{MeV}$ and cm-wide beam size. These and other similar devices, with sufficient energy to irradiate superficial tumors, are nowadays being considered for clinical trials. In contrast, the treatment of deep seated tumors at FLASH dose-rates would require much more penetrating beams. Availability of medical accelerators of charged particle beams with both high energy (high penetration depth) and high average current (UHDR) is hindered by size, complexity and cost issues, although efforts for technology development are ongoing. For instance, selected hadron therapy centers are currently capable of delivering FLASH dose-rate pencil beams and are starting to pave the way to human clinical applications.

In this context, the use of Very High Energy Electrons (VHEE), with energy in the range between 100 and 250 MeV, is considered extremely promising for clinical applications. The development of VHEE devices based on RF technology is currently actively pursued by public-private partnerships. An updated discussion of the ongoing research activity in this field can be found in[24] and in a very recent review[4]. Originally, the direct use of high energy electrons to irradiate deep seated tumors was mostly investigated via theoretical/numerical studies. Up until the beginning of 2000s, the energy range considered was limited to $\sim 50\,\mathrm{MeV}$. More recently, in light of both technology advancements in RF accelerators[25–27] and the emergence of high-gradient, laser-driven electron accelerators, dosimetric studies of VHEE beams started to be performed (see for instance[19] and Refs. therein). Monte Carlo simulations have revealed appealing features of VHEE, such as their reduced lateral spread in tissues with respect to both $\lesssim 50\,\mathrm{MeV}$ e-beams and high energy protons (also in the case of FLASH modality[28–30]); furthermore, the quality of the achievable dose conformation for some types of tumors has been shown (numerically) to be comparable or even superior to that of clinical VMAT protocols[31–33]. Moreover, the remarkable insensitivity of VHEE beams to tissue inhomogeneities has been pointed out and shown to be an added value with respect to photon and proton beams[34,35]. Other useful features offered by VHEE beams have also been recently highlighted, including the possibility of fast magnetic control, like steering to follow the patient physiological motion[36,37], or of magnetic focusing to locally enhance the delivered dose in depth, and reduce the entrance dose, or scanning, thus providing an additional degree of freedom to optimize dose conformation[37].

RT with laser-driven VHEE: Basics and main issues

In this paper we investigate the scanning of a deep seated tumor volume using a VHEE pencil beam obtained via Laser WakeField Acceleration (LWFA)[38]. The LWFA process enables very high accelerating gradients to be established in a plasma, up to 3 orders of magnitude higher than in a typical RF LINAC, thus leading to a corresponding reduction in size of the acceleration length required for a given energy. This makes laser-driven accelerators potentially very compact ("table-top") and thus very attractive for a widespread clinical use in existing hospital settings. LWFA of beams with energy from $\sim 100\,\mathrm{MeV}$s up to $\sim 10\,\mathrm{GeV}$ has been demonstrated experimentally in millimeter to few tens of centimeters long plasmas[39,40]. In particular, the VHEE energy range is nowadays routinely accessed in many ultraintense laser laboratories hosting 100 TW laser systems[41]. Recently, high stability and reproducibility of such LWFA electron beams has been demostrated[42], making laser-driven accelerators already sufficiently mature for application in RT. Furthermore, LWFA beams are intrinsically characterized by ultrashort (sub-ps) duration, which translates into beams with very high intensity and instantaneous (peak) dose rates, up to $10^{11} - 10^{13}\,\mathrm{Gy/s}$. Radiobiological consequences of this feature had been already studied in early experiments with laser-driven beams[43] and have been highlighted in most recent studies[7]. This latter study with VHEE beams identified the role of beam intensity as a key parameter in the activation of the FLASH effect, showing that the higher the dose rate, the lower the dose needed to trigger the FLASH sparing effect. These results may support FLASH operation at a small dose per fraction in the clinical setting, where fractionation remains a standard of care.

From an experimental viewpoint, efforts are ongoing to develop reliable, compact laser-driven accelerators for VHEE RT[44,45]. In parallel, dosimetric studies are being carried out with very promising results[46]. The possibility of achieving dose conformation via advanced multi-field or intensity modulation techniques, which can be seen as the building blocks for current advanced RT modalities, has been shown in[47]. Figure 1 *left* shows the dose pattern of a 7-field irradiation when targeting a deep-seated, mm-size volume in the center of a 10 cm size cylindrical phantom with a laser-driven pencil beam obtained with a similar class laser as the one considered in this work[47,48]. In a different study[49], the use of magnetic guiding based on permanent quadrupoles for pointing stabilization, transport and focusing to a phantom has been reported, providing a path to higher control of laser-driven VHEEs.

The results mentioned above, both theoretical and experimental, make a compelling case for the investigation of the dosimetric features of realistic laser-driven VHEE beams. With this respect, two aspects characterizing these beams, namely the small transverse size (few mm) and the quite large energy spread, deserve further studies, since they can strongly affect the strategies for dose pattern optimization, making these strategies potentially different from well established techniques (and algorithms) employed in current RT. In principle, both the above features can be controlled by a suitable beam conditioning. However, for the sake of pursuing a fast route toward the availability of FLASH beams with laser-driven accelerators, a pencil beam with a few millimeters of size and retaining all the charge in the available VHEE spectral range may represent an advantage. It is thus worthwhile and timely to explore the dosimetry of beams with such intrinsic features.

To this purpose, here we report on start-to-end simulations of a case study of irradiation of a brain tumor using a scanning technique, starting with a VHEE pencil beam, as suitably shaped as discussed later, which can be produced using existing, well validated LWFA acceleration regimes with 100 TW-class laser systems. We observe that theoretical/numerical works carried out so far only reported on the use of "ideal" VHEE beams, with monochromatic energy and/or large transverse size[31,50] while our study considers beam features that have been demonstrated experimentally.

As a first step toward more advanced studies, we thus consider a 1-field (i.e., one direction) irradiation of a deep seated brain tumor. While this may seem an oversimplified configuration compared to the state of the art of modern RT based on multi-field irradiation and/or intensity modulation, it is a much needed step and a building block toward more sophisticated treatment plannings. To our knowledge no similar studies have been reported so far with such realistic VHEE pencil beams. It is also worth pointing out that our study is not limited to the use of laser-driven VHEE accelerators and may be of more general relevance to VHEE beams accelerated using RF accelerators.

In the following Section, we first briefly motivate our choice of the tumor model for this case study, and the design of both the beam properties and the transport beamline. Then we report on the main findings of our study, and finally, in light of the conclusions, we discuss perspectives for LWFA-based FLASH RT.

Rationale: A brain tumor as case study of deep volume scanning with a broadband pencil beam

A brain tumor is a particularly relevant case study to start with, in light of the major advancements that a treatment exploiting the FLASH effect may potentially offer with respect to current RT protocols[51]. Primary brain tumors occur in around 300000 people per year worldwide, accounting for 3.5% of new cancer cases; in the pediatric age cohort (age 0-14) brain tumors are the second most common form of cancer[52]. Of all brain tumors, the glioblastoma (GBM) is the most common and aggressive one[53], with a median survival of 15 months[54]. Current treatment protocols involve a multi-centered approach: surgical resection, radiation therapy and chemotherapy[55]. Since very recently, immunotherapy approaches are under development, with several ongoing clinical trials (see for instance[56]). While the benefits of irradiating GBM are well established[57], the radiation induced toxicity to the healthy tissues surrounding the lesion very often leads to neurological long term adverse effects (e.g., learning and memory impairing, mood disorders, hearing loss, etc.); these effects are particularly severe for children[58,59]. In light of that, it is generally acknowledged[60] that the FLASH effect has the potential to significantly improve the risk-to-benefit ratio of RT for GBM. In particular, the healthy tissue sparing effect of a FLASH irradiation could prove essential to achieve better tumor control by increasing the delivered dose to the tumor while reducing the negative neurological side effects. *In vivo* studies carried out so far on mice showed that FLASH RT is indeed an effective treatment against brain tumors[60–62], strongly motivating investigation of VHEE accelerators in this context.

As a VHEE source, we consider a laser wakefield accelerator driven by a 100 TW-class ultrashort laser. In our study we purposefully take into account laser (power, duration, energy per pulse) and VHEE beam (energy spread, divergence and/or emittance, etc.) features already well established in medium scale laser labs worldwide, in order to keep the approach to possible clinical translation as realistic as possible. On the other hand, as it comes out from this and other studies, laser and LWFA technology developments are still required to fully exploit the FLASH effect; these points will be discussed at the end of the paper.

In the study we carried out a start-to-end simulation using a Particle-In-Cell (PIC) code to model LWFA process and a Monte Carlo code to study the beam post-acceleration manipulation, transport and interaction with a brain model. The codes used for the two purposes are briefly presented in the Materials and Methods section (M&M from now on). We refer to the Supplementary Materials (SM from now on) for further details on the LWFA accelerator and on the accelerated beam properties. Here we only mention that in our work we aimed at an acceleration regime providing a beam with most of the charge in the energy range $\sim 100-250\,\mathrm{MeV}$. We observe that, although advanced LWFA acceleration methods able to deliver lower energy spread beams than those considered here have been developed over the past decade[63–67], a trade-off exists between the energy spread and the total charge per bunch (i.e., per laser shot), which, together with the pulse repetition rate, determines the

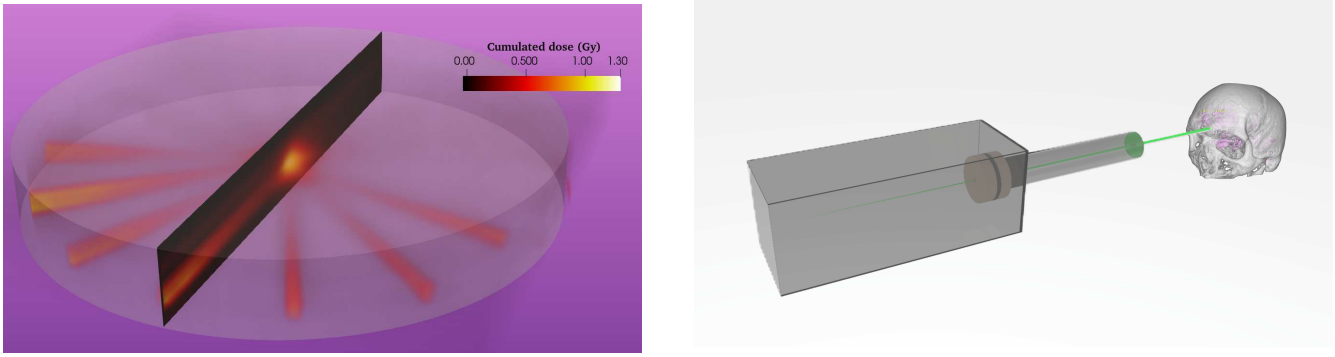


Figure 1. *Left:* 3D dose pattern obtained in a recent experiment with laser-driven VHEE beam by our group, at the Intense Laser Irradiation Laboratory of CNR-INO[48], with similar laser conditions as the ones taken into account for this work. In the experiment, the target volume was placed at the center of a 10 cm diameter cylindrical phantom and irradiated using pencil beams from 7 directions. *Right:* Sketch of the setup used for this work, which includes a collimator/shaper and a vacuum tube with a kapton exit window, followed by a 50 mm air gap to the patient. For details, see M&M.

Parameter	Nominal value
Charge per shot) with $E \geq 100$ MeV at LWFA exit	120 pC
Beam divergence (FWHM) at LWFA exit	3 mrad
Mean energy after < 100 MeV rejection	220 MeV
Charge per shot at collimator/shaper exit	50 pC
Charge per shot on patient	25 pC
Beam size (FWHM) at collimator exit	$2.5 \times 2.5\,\text{mm}^2$
Transverse size (FWHM) at buildup	$5.05\,\text{mm}^2$
Flatness at buildup	$< 6.5\%$
Dose asymmetry at buildup	$< 2\%$

Table 1. Table summarizing the main VHEE beam and dose delivery parameters and the corresponding nominal values used in this study.

ultimate average dose rate achievable. On the other hand, recent Monte Carlo simulations reported in the literature have shown a relatively weak dependence of the dose deposition pattern upon the energy spread of electrons, provided that electrons with energy $\gtrsim 100$ MeV are considered; in light of this, our acceleration regime yields a charge as high as possible, allowing the beam spectrum to span the entire VHEE range. The implications of this choice for future development of FLASH treatments, as well as the constraints on the total charge of electrons with energy lower than ~ 100 MeV, will be discussed later in the paper.

Table 1 summarizes, among others, the specifications of the VHEE beam at the exit of the plasma (accelerator stage). In particular, the bunch charge retrieved from the PIC simulations for electrons with energy > 100 MeV is of about 120 pC (the electron spectrum resulting from the PIC simulations is reported in the SM). It is worth mentioning here that a non-negligible lower energy component is in general to be expected from laser-driven accelerators. Since this component may result in a detrimental entrance dose, an energy selector to remove low energy electrons may be required. Although a discussion of such a selector is beyond the scope of this paper, we mention here that it may be obtained using a compact beamline, consisting of permanent magnets dipoles or other magnetic components, resulting in modest reduction of the charge transported at the targeted high (VHEE) energy[68]. Nevertheless, as a conservative estimate, we allow here for a 50% transport efficiency of a possible high energy pass beamline, resulting in a corresponding reduction of the charge in the VHEE range (see later and Table).

A sketch of the elements simulated in our Monte Carlo code downstream of the plasma "accelerator stage" is shown in Figure 1 *right*; the physical sizes of these elements are reported in M&M for convenience. The VHEE beam has a nearly gaussian angular shape upon exiting the plasma. In order to optimize the (transverse) dose pattern delivery, an *ad hoc* collimator, also acting as a shaper for the transverse beam profile, was designed by means of Monte Carlo simulations (see M&M). The rationale for the collimator/shaper design was the selection of a pencil beam with a sufficiently uniform transverse profile to enable a smooth coverage of the target volume, i.e., with minimal local dose overshoots in the overlapping regions between adjacent beams (see the next Section). To this purpose, we choose to select a square-shaped transverse region of the initial (LWFA exit) beam. The size of the resulting beam (see Table 1) was chosen so as to have a nearly homogeneous (this will be made more quantitative below) transverse dose pattern, while retaining the highest charge as possible. In addition, the structure

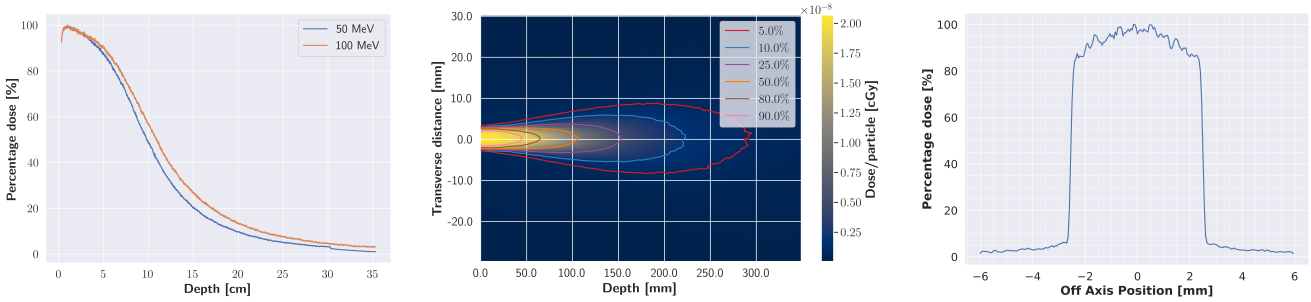


Figure 2. *Left:* Percentage Dose Depth curves for two different values of the low-energy cut, as resulting from Monte Carlo simulations. *Center:* Transverse dose distribution map, with isodose curves, for the beam considered in this work. *Right:* Transverse beamlet profile at buildup.

of the collimator was optimized so as to reduce the downstream dose contamination due to *Bremsstrahlung* photons in the X/γ-ray region. The final collimator structure is described in M&M. Upon exiting the collimator, the VHEE beam exhibits a square (flat-top) transverse profile, with the parameters shown in Table 1 (middle column). The beam is then transported in vacuum through a cylindrical pipe terminating with a kapton window (see M&M). This allows a reasonable distance to be maintained between the source and the patient, to be used for the beam steering in a real application, while ensuring that minimal perturbation to the shape of the beam occurs. Finally, a further distance in air of 50 mm was considered up to the target (either water phantom or patient).

Results

Single pencil beam dosimetry

As a first step to approach the study of a scanning procedure to cover the tumor volume, we preliminarily investigated the dosimetric features of the beam at the position of the brain model (to be presented below). To this purpose, a parallelepiped water phantom (with transverse/longitudinal size of 100/300 mm) was used. We first observe that the fraction of the original bunch charge retained after the passage through the collimator (described in M&M), vacuum pipe and window, and conservatively reduced by a factor 0.5 to allow for the usage of a low energy rejection beamline, corresponds to ~ 25 pC. In this Section, unless otherwise stated, the dose values reported refer to a single laser shot, since this is the elementary unit in the case of laser-driven accelerators.

Figure 2 *left* shows the on-axis Percentage Dose Depth (PDD) curve corresponding to two values of the lower energy cutoff of 50 MeV and 100 MeV respectively. As mentioned above, although the LWFA regime was optimized to yield most of the electron charge in the energy range greater than 100 MeV, it still exhibits a non-negligible charge at lower energy. As anticipated, a post-acceleration transport and low-energy rejection beamline is therefore needed. Although the PDD curves do not appear to dramatically differ in the two cases, electrons with energy below 100 MeV actually suffer from a higher transverse scattering both in air (i.e., on exiting the vacuum line) and within the patient brain. To minimize this we thus consider in the following an electron beam with a low energy cut at 100 MeV.

As expected for VHEE electrons the on-axis PDD exhibits a shallow maximum at a depth below 5 mm, dropping quite rapidly with depth due to the transverse scattering. In fact, as it is actually known[69], a PDD dependence on the field (that is, transverse) dimension of the beam can be observed indeed when the field size is much smaller than the penetration range of the electrons. In this condition, the lateral particle equilibrium is lost and a smaller dose is deposited along the center from particles scattered from the sides of the beam, leading to an apparent shallower dose maximum when the PDD is retrieved. Looking at the PDD curve, the R_{80} (i.e., the depth at which the dose value drops at 80% of the maximum), can be estimated to be $R_{80} \approx 70$ mm. This parameter plays a peculiar role in current protocols, as it is considered the maximum range of the beam which has therapeutic relevance in conventional radiotherapy. According to the previous considerations, however, this point deserves further investigation when dealing with mm-sized beams, as the PDD retrieved for such beams may be only partially linked to the useful depth of irradiation.

Figure 2 *center* shows a slice of the dose deposition map along a longitudinal plane. As it can be seen, the transverse size of the 5% isodose curve of the beamlet is confined within 10 mm; such a relatively low transverse spreading was already pointed out at the beginning of the 2000s, using MC simulations, for electrons with energy above ~ 100 MeV[26,70], and is essential to achieve a good dose conformation for deep seated tumors. The maximum local value of the dose is $D_{max} \simeq 2 \cdot 10^{-8}$ cGy/particle.

We refer to the final section for a deeper discussion on this point, and in particular on the possibility for laser-driven LWFA accelerators to provide FLASH VHEE beams in the near future. Finally, Figure 2 *right* shows a transverse dose profile at the position of the maximum PDD value (buildup). Following the American Association of Medical Physics task group report 25 prescriptions[71], we calculated the size, symmetry and flatness of the beamlet (see Table 1). The dose profile at z_{max} has a size of $5 \times 5\,\mathrm{mm}^2$, with flatness and symmetry deviation under 10%. Although this is already a rather good level, it may seem sub-optimal with respect to current RT standards. However, since our work is intended to establish only a first block toward more advanced dose conformation techniques with such novel pencil beams, likely using different configurations and techniques with respect to the current protocols, we cannot tackle the issue of a further optimization of these values at this stage of the work.

Brain tumor scanning dosimetry

In this subsection we present the results of the simulated irradiation of a model of a deep seated brain tumor, whose coverage was carried out with a scanning technique, using the pencil beam whose dosimetric features have been discussed above. The beamlets were sent to the patient along a common direction, which in the following will be referred to as the irradiation direction; in particular, we have chosen, for this particular study, the so-called anterior-posterior axis. The tumor was modelled as a 10 cc sphere, placed at a 80 mm depth in the CT reconstructed head of a male patient, toward the upper part of the brain (this is a quite common position for GBM, for instance); from now on, as it is customary, we will refer to this sphere as the Planned Target Volume (PTV). Figure 3 shows the 3D views of our model, with the PTV highlighted in red. Details on the CT model and the DICOM image file management can be found in M&M.

The scanning technique (namely, the total number and positioning of beamlets) was designed with the following two objectives, both to be accomplished on the proximal target projection plane (that is, the plane touching the PTV, normal to the beams direction and closer to the source): a) let neighbor beamlets to "touch" each other, that is to cover the entire plane with minimal overlapping on this plane; b) make each point of the entire PTV cross section to be covered by at least one beamlet. This procedure resulted in a total of 50 beamlets needed to cover the PTV.

Figure 4 shows the dose maps as resulting from this pencil beam scanning. We first observe that our procedure leads to unwanted dose overshoots, upstream of the PTV, where overlapping among the dose from neighbor beamlets occurs. As a better estimate of this effect, we can refer to Figure 5 *left*, where two lineouts of the dose pattern are shown, taken on two transverse (i.e., perpendicular to the original beams direction) planes, namely the proximal plane of the brain (thus inside the skull vault) and the proximal plane of the PTV. On the first plane, the maximum dose across overlapping regions could be estimated to reach a maximum value of $\sim 119\%$ of the dose along the center of each beamlet. These dose "spikes" are a direct consequence of our choice of the coverage condition on the proximal plane of the PTV and are peculiar of the usage of pencil beams with such a small size to cover the PTV; tackling this point will require further advancements in the pencil beam shaping and underlying scanning algorithm. Furthermore, as also visible in Figure 5 *left*, despite condition a) above, the requirement for each PTV proximal plane point to be covered by at least one beamlet (condition b)), coupled to the spreading occurring along the propagation up to the PTV, leads to a slight transverse modulation of the dose, with spikes reaching a value up to $\sim 105\%$ of the dose in the valleys; it is easily understood that, although this is a similar problem to what one can encounter in current photon-based protocols, the usage of pencil beams, while opening room for very precise dose delivery, makes the quest for advanced optimization algorithms and techniques very stringent.

Within the PTV itself, on the other hand, Figure 4 shows a qualitatively well-covered target, with no major cold spots across the volume. The corresponding DVH (Figure 5 *right*, discussed below) allows this coverage and homogeneity to be quantified: normalizing the dose distribution to cover 95% of the target volume with 95% of an arbitrary prescription dose, we obtain $D_{mean} \approx 98\%$ and $D_{0.35cc} \approx 110\%$, indicating a good level of target coverage and homogeneity despite the deep location of the PTV, nearly at the center of the head.

It is also worth observing that the dose transverse spread is limited to a few millimeters from the centers of the most external beamlets; this is strictly related to the usage of VHEE beams, whose well known advantage in terms of reduced transverse scattering is preserved in our pencil beam scan pattern.

Finally, all the previous observations are summed up in the Dose Volume Histogram shown in Figure 5 *right*. Beside the PTV, three more regions of interest were identified, namely the whole head, the whole brain, and an anterior-posterior section of the brain hosting the PTV, centered at the geometrical center of the PTV itself and extending beyond its edges for 20 mm in the horizontal direction and for 10 mm in the vertical one (see Figure 4); the latter volume allows a better assessment of the lateral dose spread as well as of the unwanted dose in the proximal area. Beside a conventional radiation treatment, we also consider here the possible contribution of the FLASH effect. An established custom approach here consists in using a FLASH "dose modifying factor" (DMF) (see for instance[50] and Refs. therein); in our case, we consider a conservative value DMF $= 0.80$. The DVH was normalized in order to obtain a 95% PTV volume coverage with 95% of the deposited dose. From the DVH

we can deduce that, thanks to the scanning with our square shape pencil beams, the dose was well conformed on the target. The volume with the second highest coverage was the *ad hoc* brain section volume created around the PTV. In this volume, in particular, we obtained a region irradiated with a relatively high amount of dose, with a D_{max} of the order of within 5% of the PTV maximum dose. It is worth noticing, however, that, as it can be seen from the corresponding curves with DMF $= 0.8$, taking into account a sparing due to the FLASH effect greatly improves the quality of these DVH, even in spite of the fact that we are actually considering here a higher (i.e., lower sparing) DMF value with respect to what is emerging from recent experiments[72].

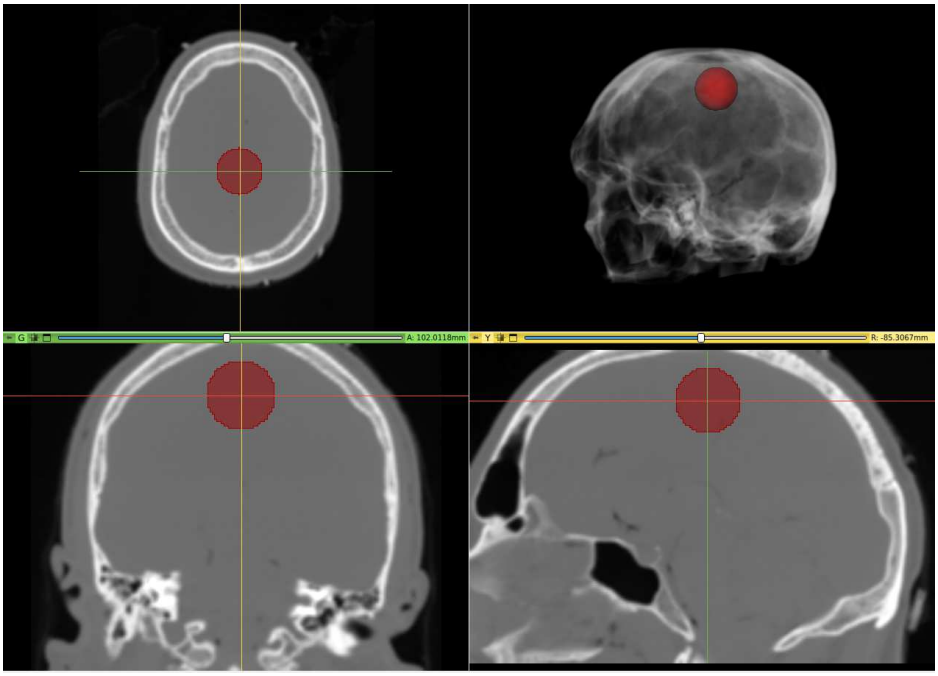


Figure 3. Ad hoc placed tumor volume (red sphere of $\sim$10 cc) in the reconstructed CT volume; projections and 3D view.

Perspectives for laser-driven VHEE RT and open issues

The results presented above clearly show the potential of a realistic laser-driven VHEE pencil beam for the irradiation of a deep-seated brain tumor via a scanning procedure, after a suitable shaping, with a square aperture collimator, in the transverse plane. Although no attempt has been made here to optimize the dose pattern via multi-field conformation techniques, our study provides a much needed building block for future, more elaborated treatments. In particular, it is worth emphasizing that, to our knowledge, this is the first work in which the dosimetry in a synthetic phantom of VHEE beams with both relatively broad spectrum and small transverse size has been investigated numerically. Our work was mostly motivated by, and designed upon, the usage of realistic laser-driven VHEE beams subject to a relatively "noninvasive" beam conditioning and, in principle, a higher charge per bunch to be transported to the patient, with a resulting higher dose rate with respect to monochromatic beams.

The resulting overall performance as obrained from our study looks promising and instructive, in view of the improvements that are expected to be made possible by advanced conformation techniques. In particular, the ballistics of the beam appears very good, providing a first indication that a quite broad spectrum can be compatible with real treatments; from this point of view, it is worth stressing that the rather important dose contribution at the entrance is expected to be much smoothed out using, for instance, multi-field irradiation, very much as in the case of current VMAT technology. One of the issues emerging from our study pertains to the dose overshoot in the overlapping regions among neighbor beamlets; this is closely related to the usage of small transverse size beams, peculiar of laser-driven VHEE beams. With this respect , smarter approaches may be elaborated with respect to the one adopted here, where a relatively gross padding on the proximal plane was planned. This is of a particular relevance in view of the increasing role that pencil particle beams are expected to play in the context of FLASH RT[7]. It is worth mentioning at this point that a major difference exists between VHEE and photon beams with respect to the dose transverse spreading, whose effect on the methods to cover a PTV with adjacent pencil beams have to be better investigated.

Furthermore, as anticipated above, the usage of the PDD (and the quantities derived from that) as a figure of merit of very small size VHEE beams has to be deepened; indeed, while the loss of the transverse equilibrium that leads to a reduced R_{80} is

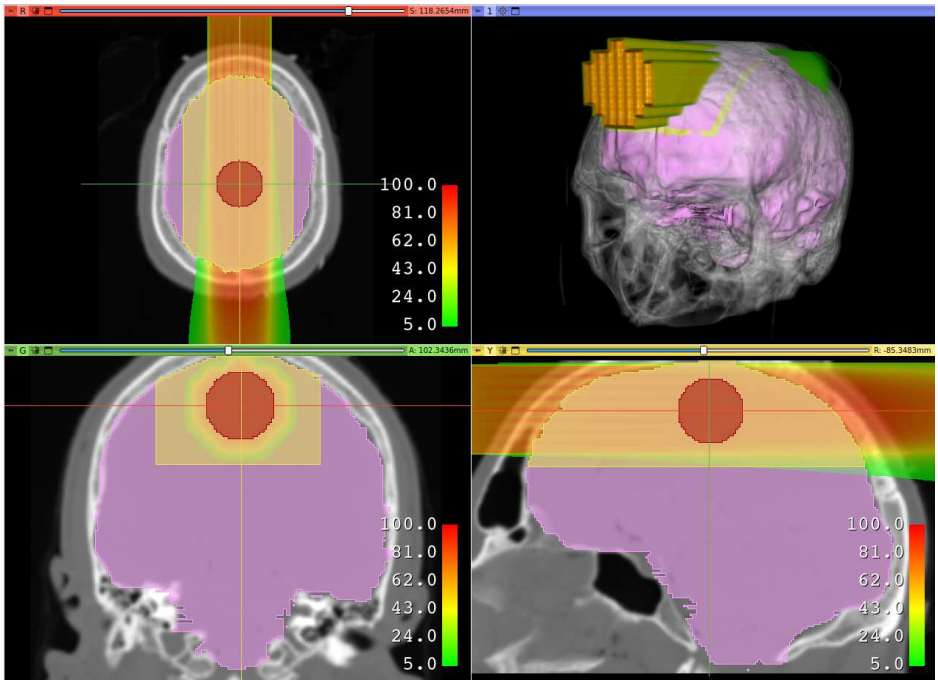


Figure 4. Dose deposition of the pencil beam scanning simulation. PTV and organs-at-risks segmentations are superimposed to the CT image.

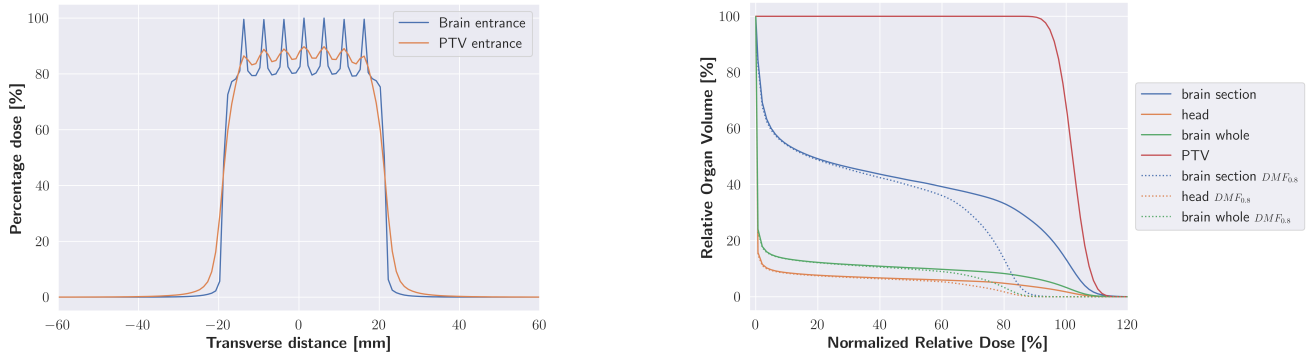


Figure 5. *Left:* Lineout of the dose deposition profiles along two planes perpendicular to the incoming beams direction: the proximal plane of the brain (blue curve) and the proximal plane of the PTV (red curve). *Right:* Dose Volume Histogram calculated for different volumes (see text and Figure 4.)

already well known, new figures need to be identified to evaluate the ability of a beam to treat deep seated tumors, as shown by this work, where a PTV well beyond the "conventional" R_{80} depth was covered, and with a dose deposited in the volume closely surrounding the PTV much lower than the one which might have been guessed by just looking at the PDD curve.

In addition to all these considerations, it is clear that the exploitation of the FLASH effect is a strong motivation for developing laser-driven VHEE accelerators. As it appears from the DVHs we have shown here, taking into account healthy tissue sparing due to the FLASH effect greatly improves the irradiation outcome, even in the rather simplified irradiation geometry considered here. In this respect, we mention that more accurate consideration of the FLASH effect may be introduced in the DVH calculations with respect to the one used here, such as, for instance, a tissue/organ-dependent DMF or a local dose threshold for the onset of the effect. However, this is a rather challenging issue at this stage, since studies of the biology underpinning the effect are ongoing and questions are still open. On the other hand, it is worth reminding that the value of the DMF we have used above is rather conservative, in light of existing studies (see for instance[72] and Refs. therein).

Finally, we wish to briefly discuss perspectives for real FLASH-ready VHEE sources based on LWFA to become available.

We preliminarily observe that laser-driven VHEE beams are intrinsically characterized by an ultrashort bunch duration, making their *instantaneous* dose rate reaching ultrahigh values, typically exceeding $10^{11} - 10^{12}\,\mathrm{Gy/s}$; whether this is enough to result in a FLASH-like sparing is an ongoing subject of investigation (see for instance[9] or[6]). Beside this rather unique feature, laser-driven electron accelerators are considered among the most promising sources for UHDR treatments of deep seated tumors, due to their potential for delivering VHEE beams with high peak current, while maintaining, as mentioned in the Introduction, the small footprint of the accelerating structure (the plasma). This translates into a very compact size, compatible with a widespread deployment in hospitals, as they require, for instance, less bulky radioprotection shieldings, and/or exhibit more affordable deployment and maintenance costs.

A major effort is ongoing to further develop and engineer LWFA accelerators for VHEE and FLASH radiotherapy, motivating the establishment of dedicated projects at major laser laboratories, including the Extreme Light Infrastructure[73]. Two major lines of development are currently actively pursued, pertaining the increase of the electron charge per bunch (laser shot) and the increase of the laser repetition rate. As for the first, developments concern the enhancement of single bunch properties aimed at increasing bunch charge while keeping energy spread and emittance at the levels required for proper beam transport and focusing using dipoles, quadrupoles or sextupoles (see for instance[74]). Indeed, differently from photons, VHEE beams with modest quality can be easily focused to achieve localized dose deposition, with reduced dose at the entrance and at the organs at risk surrounding the tumor. This may potentially lead to a figure of merit somewhat similar to the case of Bragg peak with protons or light ions, but without the instrumental complexity of a hadron therapy system and with much reduced sensitivity to tissue inhomogeneities along the beam path. As it comes out from this study, with the values of charge per bunch (i.e., per laser shot) typical of the LWFA experiments carried out so far, lying in the range from a few tens up to a few hundreds of pC, the typical dose value per shot ranges from a few cGy to several tens of cGy. Recent experiments with nano-particle assisted LWFA have already demonstrated nC-level total charge[75] at even larger energies than VHEE. On the other hand, a better energy spread control is mainly linked to the control of electron injection, which is a highly advanced area of investigation. Studies aimed at this optimization having in mind FLASH application of LWFA are needed and increasing effort is ongoing.

At the same time, engineering of scientifically established LWFA sources is mainly aimed at increasing the pulse repetition rate to meet the VHEE and FLASH constraint and ensure a stable and reproducible beam generation. In fact, delivering a therapeutic dose of $\mathcal{O}(10\,\mathrm{Gy})$ for VHEE radiotherapy requires accumulation of hundreds of laser shots whose statistical properties are crucial to ensure compliance with radiotherapy standards. Moreover, in the case of FLASH radiotherapy, delivering the above dose in the time window required for activation of the FLASH effect, of the order of few hundreds of milliseconds, requires a high operational repetition rate of LWFA, $\mathcal{O}(100\,\mathrm{Hz})$ or above. So far, kHz repetition rate LWFA has been demonstrated with beam energy up to tens of MeV scale[76,77], while for VHEE beams the demonstrated repetition rate is limited to lower values, around 1 to 10 Hz. Such limitation is mainly due to the available industrial laser systems, whose repetition rate for the pulse energy required for VHEE beams has been limited to 10 Hz or less. This paradigm is now changing, with the implementation of diode-pumping laser technology. Titanium-Sapphire based systems operating at Joule energy level per pulse and 100 Hz repetition rate have been recently developed[78], and are now available, specifically designed for the scope of VHEE radiotherapy research and other industrial applications requiring high average laser power. At the same time, fully diode-pumped systems with new lasing materials are being demonstrated for efficient operation at the kHz repetition rate without the limitations on pulse energy of kHz systems available today. Engineering developments also include gas target systems operating at a higher repetition rate or in CW, to enable LWFA operation at 100 Hz and above. Established solutions for gas target systems already exist at an industrial level with quasi-continuous performance enabling kHz operation of LWFA accelerator, currently demonstrated at the 10 MeV electron energy. These performances, combined with the intrinsic UHDR pulses of LWFA make the case study of pencil beam LWFA VHEE accelerators presented here timely and highly relevant for the establishment of novel RT approaches.

Materials and methods

LWFA stage: PIC simulations

The laser-plasma interaction was simulated using the Particle-In-Cell (PIC) code FBPIC[79]; this code implements a pseudo-spectral, quasi-cylindrical PIC algorithm (see SM for further details). The driver laser, featuring a 3 J energy, 30 fs pulse duration, was focused at an intensity of $I \simeq 1.6 \times 10^{19}\,\mathrm{W/cm^2}$ ($a_0 \simeq 2.7$) onto a 3 mm long gas-jet target, made up by a mixture of He (99%) and Ar (1%). The background electron density was tailored, after a parametric study, so that the LWFA process, occurring in the so-called "bubble" regime, yielded most of the charge in the $100-250$MeV energy range; the electron density resulting from this study was $n_e \simeq 9.4 \times 10^{17}$. In the acceleration regime selected, most of the accelerated electrons were seen to come from ionization injection of electrons born out of the Ar 12+ ion species, which allowed the total charge of electrons with $E \lesssim 50\,\mathrm{MeV}$ to be minimized. The two dimensional ($z-r$, being z and r the longitudinal and transverse coordinates,

Parameter	Value
LWFA to collimator/shaper entrance distance	380 mm
Collimator/shaper depth	47.5 mm
LWFA to tube entrance distance	30 mm
Tube (vacuum extension) depth	300 mm
Vacuum-air feedthrough (window) material and thickness	*kapton*™, 20 μm
Window to patient distance	50 mm

Table 2. Table summarizing the main parameters of the simulated geometry.

respectively) simulation box considered is a moving window with size $75 \times 48\,\mu m^2$ and spatial resolution $0.025 \times 0.08\,\mu m^2$ (corresponding to a sampling of 32×10 points per λ). The field expansion in azimuthal modes was truncated to second order, and the time resolution was $\Delta t = 0.08$ fs, with a total time of $T \simeq 10$ ps.

VHEE beam dosimetry and tumor scanning: Monte Carlo simulations and experimental benchmarking

The transport and dosimetric properties of the laser-driven VHEE beam obtained by the PIC simulations were studied using a homemade code based on the GEANT4 toolkit (version 10.7p3)[80–82]. The same code, which features multi-threading capabilities and is equipped with a DICOM file importing routine, was used to study and optimize the PTV scanning procedure in the brain model. Transport and interactions of the particles were simulated using the QBBC physics list with the electromagnetic physics constructor 4, the most accurate for low energy particle transport; the particle range was set to 100 μm in all regions. The primary particles phase space was generated by an inversion sampling method applied to the energy and angular distributions obtained from the PIC simulations. A total of up to 10^7 primary particles were typically used for each run.

The study of the PTV scanning technique with our laser-driven pencil beams was performed using a real head region CT of a male patient taken from the Visible Human Project database[83]. The DICOM CT file hosted an axial CT reconstructed head, which was imported in the code as a set of cubic, 1 mm^3 size voxels. Code-wise, this was achieved using a concrete C++ instance of the `G4VNestedParameterisation` virtual class, with noticeable memory saving with respect to a standard parameterisation. The scored quantity was the deposited dose; the dose tally was performed on voxels of $0.5 \times 0.5 \times 0.2$ and $0.1 \times 0.1 \times 0.1\,mm^3$ for the calculation of the PDD and of the beam profile, respectively, while the entire voxel was used for the patient head.

Simulation geometry and collimator features

A sketch of the simulated geometry is shown in Figure 1 *right*, discussed in the text. Table 2 reports the main geometrical parameters considered.

The collimator/shaper, whose assembly was a 47.5 mm thick, 80 mm diameter cylinder, was made up by a sandwich of 3 cylinders of different materials, namely a 20 mm thick PMMA layer, a 7.5 mm thick lead layer, and a 20 mm thick PMMA layer. At the center of this structure, a square aperture was considered, having a 2.5 mm size. Surrounding this aperture, a 1.25 mm PMMA layer was considered along the 4 sides.

Data availability

The authors can provide the code sources and data used for this work upon reasonable request.

References

1. Zhu, H. *et al.* Global radiotherapy demands and corresponding radiotherapy-professional workforce requirements in 2022 and predicted to 2050: a population-based study. *The Lancet Glob. Heal.* **12**, e1945–e1953 (2024).
2. Chen, H. *et al.* Radiotherapy modulates tumor cell fate decisions: a review. *Radiat. Oncol.* **17**, 196, DOI: 10.1186/s13014-022-02171-7 (2022).
3. Favaudon, V. *et al.* Ultrahigh dose-rate flash irradiation increases the differential response between normal and tumor tissue in mice. *Sci. Transl. Medicine* **6**, 245ra93–245ra93, DOI: 10.1126/scitranslmed.3008973 (2014). https://www.science.org/doi/pdf/10.1126/scitranslmed.3008973.
4. Panaino, C. M. V. *et al.* Very high-energy electron therapy toward clinical implementation. *Cancers* **17**, DOI: 10.3390/cancers17020181 (2025).

5. Vozenin, M.-C., Hendry, J. H. & Limoli, C. Biological benefits of ultra-high dose rate flash radiotherapy: sleeping beauty awoken. *Clin. oncology* **31**, 407–415 (2019).
6. Vozenin, M.-C. *et al.* Flash: New intersection of physics, chemistry, biology, and cancer medicine. *Rev. Mod. Phys.* **96**, 035002, DOI: 10.1103/RevModPhys.96.035002 (2024).
7. Kacem, H. *et al.* Modification of the microstructure of the cern-clear-vhee beam at the picosecond scale modifies zfe morphogenesis but has no impact on hydrogen peroxide production. *Radiother. Oncol.* **209**, DOI: 10.1016/j.radonc.2025.110942 (2025).
8. Kacem, H., Almeida, A., Cherbuin, N. & Vozenin, M.-C. Understanding the FLASH effect to unravel the potential of ultra-high dose rate irradiation. *Int. J. Radiat. Biol.* **98**, 506–516, DOI: 10.1080/09553002.2021.2004328 (2022).
9. Friedl, A. A., Prise, K. M., Butterworth, K. T., Montay-Gruel, P. & Favaudon, V. Radiobiology of the FLASH effect. *Med. Phys.* **49**, 1993–2013, DOI: 10.1002/mp.15184 (2022).
10. McGarrigle, J. M., Long, K. R. & Prezado, Y. The flash effect—an evaluation of preclinical studies of ultra-high dose rate radiotherapy. *Front. Oncol.* **14**, 1340190 (2024).
11. Borghini, A. *et al.* Flash ultra-high dose rates in radiotherapy: preclinical and radiobiological evidence. *Int. J. Radiat. Biol.* **98**, 127–135, DOI: 10.1080/09553002.2022.2009143 (2022). PMID: 34913413, https://doi.org/10.1080/09553002.2022.2009143.
12. Borghini, A. *et al.* Flash radiotherapy: Expectations, challenges, and current knowledge. *Int. J. Mol. Sci.* **25**, 2546, DOI: 10.3390/ijms25052546 (2024).
13. Chow, J. C. L. & Ruda, H. E. Mechanisms of action in flash radiotherapy: A comprehensive review of physicochemical and biological processes on cancerous and normal cells. *Cells* **13**, 835, DOI: 10.3390/cells13100835 (2024).
14. Rosini, G., Ciarrocchi, E. & D'Orsi, B. Mechanisms of the flash effect: Current insights and advances. *Front. Cell Dev. Biol.* **13**, 1575678, DOI: 10.3389/fcell.2025.1575678 (2025).
15. Wilson, J. D., Hammond, E. M., Higgins, G. S. & Petersson, K. Ultra-High Dose Rate (FLASH) Radiotherapy: Silver Bullet or Fool's Gold? *Front. Oncol.* **9**, 1563, DOI: 10.3389/fonc.2019.01563 (2020).
16. Sampayan, S. E. *et al.* Megavolt bremsstrahlung measurements from linear induction accelerators demonstrate possible use as a FLASH radiotherapy source to reduce acute toxicity. *Sci. Reports* **11**, 17104, DOI: 10.1038/s41598-021-95807-9 (2021).
17. Esplen, N., Mendonca, M. S. & Bazalova-Carter, M. Physics and biology of ultrahigh dose-rate (FLASH) radiotherapy: a topical review. *Phys. Medicine & Biol.* **65**, 23TR03, DOI: 10.1088/1361-6560/abaa28 (2020).
18. Bourhis, J. *et al.* Treatment of a first patient with flash-radiotherapy. *Radiother. oncology* **139**, 18–22 (2019).
19. Ronga, M. G. *et al.* Back to the Future: Very High-Energy Electrons (VHEEs) and Their Potential Application in Radiation Therapy. *Cancers* **13**, 4942, DOI: 10.3390/cancers13194942 (2021).
20. Righi, S., Karaj, E., Felici, G. & Di Martino, F. Dosimetric characteristics of electron beams produced by two mobile accelerators, Novac7 and Liac, for intraoperative radiation therapy through Monte Carlo simulation. *J. Appl. Clin. Med. Phys.* **14**, 6–18, DOI: 10.1120/jacmp.v14i1.3678 (2013).
21. Lempart, M. *et al.* Modifying a clinical linear accelerator for delivery of ultra-high dose rate irradiation. *Radiother. Oncol.* **139**, 40–45, DOI: 10.1016/j.radonc.2019.01.031 (2019).
22. Rahman, M. *et al.* Electron FLASH Delivery at Treatment Room Isocenter for Efficient Reversible Conversion of a Clinical LINAC. *Int. J. Radiat. Oncol.* **110**, 872–882, DOI: 10.1016/j.ijrobp.2021.01.011 (2021).
23. Felici, G. *et al.* Transforming an IORT Linac Into a FLASH Research Machine: Procedure and Dosimetric Characterization. *Front. Phys.* **8**, 374, DOI: 10.3389/fphy.2020.00374 (2020).
24. Farr, J., Grilj, V., Malka, V., Sudharsan, S. & Schippers, M. Ultra-high dose rate radiation production and delivery systems intended for FLASH. *Med. Phys.* **49**, 4875–4911, DOI: 10.1002/mp.15659 (2022).
25. DesRosiers, C., Moskvin, V., Bielajew, A. F. & Papiez, L. 150-250 MeV electron beams in radiation therapy. *Phys. Medicine Biol.* **45**, 1781–1805, DOI: 10.1088/0031-9155/45/7/306 (2000).
26. Yeboah, C., Sandison, G. A. & Moskvin, V. Optimization of intensity-modulated very high energy (50–250 MeV) electron therapy. *Phys. Medicine Biol.* **47**, 1285–1301, DOI: 10.1088/0031-9155/47/8/305 (2002).
27. Palma, B. *et al.* Assessment of the quality of very high-energy electron radiotherapy planning. *Radiother. Oncol.* **119**, 154–158, DOI: 10.1016/j.radonc.2016.01.017 (2016).

28. Muscato, A. *et al.* Treatment planning of intracranial lesions with vhee: comparing conventional and flash irradiation potential with state-of-the-art photon and proton radiotherapy. *Front. Phys.* **11**, DOI: 10.3389/fphy.2023.1185598 (2023).

29. Böhlen, T. T. *et al.* Very high-energy electron therapy as light-particle alternative to transmission proton flash therapy – an evaluation of dosimetric performances. *Radiother. Oncol.* **194**, 110177, DOI: 10.1016/j.radonc.2024.110177 (2024).

30. Gesualdi, F. *et al.* Comparison of protons and very high-energy electrons transmission pencil-beam-scanning for flash radiotherapy. *Phys. Radiat. Oncol. (PHRO)* DOI: 10.1016/j.phro.2025.100860 (2025). Transmission proton and VHEE PBS treatment plan comparison with dose rate quantification relevant to FLASH radiotherapy.

31. Bazalova-Carter, M. *et al.* Treatment planning for radiotherapy with very high-energy electron beams and comparison of VHEE and VMAT plans. *Med. Phys.* **42**, 2615–2625, DOI: 10.1118/1.4918923 (2015).

32. Fuchs, T. *et al.* Treatment planning for laser-accelerated very-high energy electrons. *Phys. Medicine Biol.* **54**, 3315–3328, DOI: 10.1088/0031-9155/54/11/003 (2009).

33. Rahman, M. *et al.* FLASH radiotherapy treatment planning and models for electron beams. *Radiother. Oncol.* **175**, 210–221, DOI: 10.1016/j.radonc.2022.08.009 (2022).

34. Lagzda, A. *et al.* Influence of heterogeneous media on Very High Energy Electron (VHEE) dose penetration and a Monte Carlo-based comparison with existing radiotherapy modalities. *Nucl. Instruments Methods Phys. Res. Sect. B: Beam Interactions with Mater. Atoms* **482**, 70–81, DOI: 10.1016/j.nimb.2020.09.008 (2020).

35. DesRosiers, C., Moskvin, V., Cao, M., Joshi, C. J. & Langer, M. Laser-plasma generated very high energy electrons in radiation therapy of the prostate. 688109, DOI: 10.1117/12.761663 (San Jose, CA, 2008).

36. Maxim, P. G., Tantawi, S. G. & Loo, B. W. PHASER: A platform for clinical translation of FLASH cancer radiotherapy. *Radiother. Oncol.* **139**, 28–33, DOI: 10.1016/j.radonc.2019.05.005 (2019).

37. Kokurewicz, K. *et al.* Focused very high-energy electron beams as a novel radiotherapy modality for producing high-dose volumetric elements. *Sci. Reports* **9**, 10837, DOI: 10.1038/s41598-019-46630-w (2019).

38. Esarey, E., Schroeder, C. B. & Leemans, W. P. Physics of laser-driven plasma-based electron accelerators. *Rev. Mod. Phys.* **81**, 1229–1285, DOI: 10.1103/RevModPhys.81.1229 (2009).

39. Gonsalves, A. *et al.* Petawatt Laser Guiding and Electron Beam Acceleration to 8 GeV in a Laser-Heated Capillary Discharge Waveguide. *Phys. Rev. Lett.* **122**, 084801, DOI: 10.1103/PhysRevLett.122.084801 (2019).

40. Picksley, A. *et al.* Matched guiding and controlled injection in dark-current-free, 10-gev-class, channel-guided laser-plasma accelerators. *Phys. Rev. Lett.* **133**, 255001, DOI: 10.1103/PhysRevLett.133.255001 (2024).

41. Danson, C. N. *et al.* Petawatt and exawatt class lasers worldwide. *High Power Laser Sci. Eng.* **7**, e54, DOI: 10.1017/hpl.2019.36 (2019).

42. Maier, A. R. *et al.* Decoding Sources of Energy Variability in a Laser-Plasma Accelerator. *Phys. Rev. X* **10**, 031039, DOI: 10.1103/PhysRevX.10.031039 (2020).

43. Giulietti, A. (ed.) *Laser-Driven Particle Acceleration Towards Radiobiology and Medicine*. Biological and Medical Physics, Biomedical Engineering (Springer International Publishing, Cham, 2016).

44. Li, H. *et al.* Design of a 100-mev compact vhee beam line in tsinghua university. *Front. Phys.* **12**, DOI: 10.3389/fphy.2024.1496272 (2025).

45. Guo, Z. *et al.* Preclinical tumor control with a laser-accelerated high-energy electron radiotherapy prototype. *Nat. Commun.* **16**, 1895, DOI: 10.1038/s41467-025-57122-z (2025).

46. Giaccaglia, C. *et al.* Multiscale radiobiological assessment of laser-driven very high energy electrons versus conventional electrons. *Adv. Radiat. Oncol.* **11**, 102028, DOI: https://doi.org/10.1016/j.adro.2026.102028 (2026).

47. Labate, L. *et al.* Toward an effective use of laser-driven very high energy electrons for radiotherapy: Feasibility assessment of multi-field and intensity modulation irradiation schemes. *Sci. Reports* **10**, 17307, DOI: 10.1038/s41598-020-74256-w (2020).

48. Gizzi, L. A. *et al.* Overview and specifications of laser and target areas at the Intense Laser Irradiation Laboratory. *High Power Laser Sci. Eng.* **9**, e10, DOI: 10.1017/hpl.2020.47 (2021).

49. Svendsen, K. *et al.* A focused very high energy electron beam for fractionated stereotactic radiotherapy. *Sci. Reports* **11**, 5844, DOI: 10.1038/s41598-021-85451-8 (2021).

50. Sarti, A. *et al.* Deep Seated Tumour Treatments With Electrons of High Energy Delivered at FLASH Rates: The Example of Prostate Cancer. *Front. Oncol.* **11**, 777852, DOI: 10.3389/fonc.2021.777852 (2021).

51. Mann, J., Ramakrishna, R., Magge, R. & Wernicke, A. G. Advances in Radiotherapy for Glioblastoma. *Front. Neurol.* **8**, 748, DOI: 10.3389/fneur.2017.00748 (2018).

52. Sung, H. *et al.* Global cancer statistics 2020: Globocan estimates of incidence and mortality worldwide for 36 cancers in 185 countries. *CA: A Cancer J. for Clin.* **71**, 209–249, DOI: https://doi.org/10.3322/caac.21660 (2021).

53. Louis, D. N. *et al.* The 2016 world health organization classification of tumors of the central nervous system: a summary. *Acta neuropathologica* **131**, 803–820 (2016).

54. Koshy, M. *et al.* Improved survival time trends for glioblastoma using the seer 17 population-based registries. *J. neuro-oncology* **107**, 207–212 (2012).

55. Stupp, R. *et al.* Radiotherapy plus concomitant and adjuvant temozolomide for glioblastoma. *New Engl. journal medicine* **352**, 987–996 (2005).

56. Liu, Y., Zhou, F., Ali, H., Lathia, J. D. & Chen, P. Immunotherapy for glioblastoma: current state, challenges, and future perspectives. *Cell. & Mol. Immunol.* **21**, 1354–1375, DOI: 10.1038/s41423-024-01226-x (2024).

57. Barani, I. J. & Larson, D. A. Radiation therapy of glioblastoma. *Curr. understanding treatment gliomas* 49–73 (2015).

58. DeNunzio, N. J. & Yock, T. I. Modern radiotherapy for pediatric brain tumors. *Cancers* **12**, 1533 (2020).

59. Butler, J. M., Rapp, S. R. & Shaw, E. G. Managing the cognitive effects of brain tumor radiation therapy. *Curr. treatment options oncology* **7**, 517–523 (2006).

60. Montay-Gruel, P. *et al.* Hypofractionated flash-rt as an effective treatment against glioblastoma that reduces neurocognitive side effects in mice. *Clin. Cancer Res.* **27**, 775–784 (2021).

61. Montay-Gruel, P. *et al.* Irradiation in a flash: Unique sparing of memory in mice after whole brain irradiation with dose rates above 100 gy/s. *Radiother. Oncol.* **124**, 365–369 (2017).

62. Alaghband, Y. *et al.* Neuroprotection of radiosensitive juvenile mice by ultra-high dose rate flash irradiation. *Cancers* **12**, 1671 (2020).

63. Pollock, B. B. *et al.* Demonstration of a Narrow Energy Spread, ~0.5 GeV Electron Beam from a Two-Stage Laser Wakefield Accelerator. *Phys. Rev. Lett.* **107**, 045001, DOI: 10.1103/PhysRevLett.107.045001 (2011).

64. Buck, A. *et al.* Shock-Front Injector for High-Quality Laser-Plasma Acceleration. *Phys. Rev. Lett.* **110**, 185006, DOI: 10.1103/PhysRevLett.110.185006 (2013).

65. Gonsalves, A. J. *et al.* Tunable laser plasma accelerator based on longitudinal density tailoring. *Nat. Phys.* **7**, 862–866, DOI: 10.1038/nphys2071 (2011).

66. Thaury, C. *et al.* Shock assisted ionization injection in laser-plasma accelerators. *Sci. Reports* **5**, 16310, DOI: 10.1038/srep16310 (2015).

67. Tomassini, P. *et al.* High quality electron bunches for a multistage GeV accelerator with resonant multipulse ionization injection. *Phys. Rev. Accel. Beams* **22**, 111302, DOI: 10.1103/PhysRevAccelBeams.22.111302 (2019).

68. Kalvala, R. *et al.* Start-to-end modelling of laser-plasma acceleration, beam transport and dose deposition of very high-energy electrons for radiotherapy. *Sci. Reports* DOI: 10.1038/s41598-026-49116-8 (2026).

69. Gibbons, J. *Khan's The Physics of Radiation Therapy* (Wolters Kluwer Health, Lippincott Williams & Wilkins, 2019), 6th edn.

70. Papiez, L., DesRosiers, C. & Moskvin, V. Very High Energy Electrons (50 – 250 MeV) and Radiation Therapy. *Technol. Cancer Res. & Treat.* **1**, 105–110, DOI: 10.1177/153303460200100202 (2002).

71. Khan, F. M. *et al.* Clinical electron-beam dosimetry: Report of AAPM Radiation Therapy Committee Task Group No. 25. *Med. Phys.* **18**, 73–109, DOI: 10.1118/1.596695 (1991).

72. Böhlen, T. T. *et al.* Normal Tissue Sparing by FLASH as a Function of Single-Fraction Dose: A Quantitative Analysis. *Int. J. Radiat. Oncol.* **114**, 1032–1044, DOI: 10.1016/j.ijrobp.2022.05.038 (2022).

73. Hideghéty, K. *et al.* From ultrafast laser-generated radiation to clinical impact: a roadmap for radiobiology and cancer research at the extreme light infrastructure (eli). *The Eur. Phys. J. Plus* **140**, 730, DOI: 10.1140/epjp/s13360-025-06662-w (2025).

74. Gajdos, P. & Krus, M. Ultrashort electron beam isochronous, achromatic transport line design. In Bulanov, S. S., Schreiber, J. & Schroeder, C. B. (eds.) *Laser Acceleration of Electrons, Protons, and Ions VI*, vol. 11779, 117790G, DOI: 10.1117/12.2589208. International Society for Optics and Photonics (SPIE, 2021).

75. Aniculaesei, C. *et al.* The acceleration of a high-charge electron bunch to 10 GeV in a 10-cm nanoparticle-assisted wakefield accelerator. *Matter Radiat. at Extrem.* **9**, 014001, DOI: 10.1063/5.0161687 (2023).

76. Rovige, L. *et al.* Demonstration of stable long-term operation of a kilohertz laser-plasma accelerator. *Phys. Rev. Accel. Beams* **23**, 093401, DOI: 10.1103/PhysRevAccelBeams.23.093401 (2020).

77. Lazzarini, C. M. *et al.* Controlled khz laser-driven electron irradiations for pre-clinical applications (2026). 2603.10058.

78. Kabacinski, A. *et al.* High average power room temperature laser based on a 300-mj 100-hz ti:sa disk amplifier. *Opt. Lett.* **50**, 5630–5633, DOI: 10.1364/OL.569969 (2025).

79. Lehe, R., Kirchen, M., Andriyash, I. A., Godfrey, B. B. & Vay, J.-L. A spectral, quasi-cylindrical and dispersion-free particle-in-cell algorithm. *Comput. Phys. Commun.* **203**, 66–82, DOI: https://doi.org/10.1016/j.cpc.2016.02.007 (2016).

80. Agostinelli, S. *et al.* Geant4—a simulation toolkit. *Nucl. Instruments Methods Phys. Res. Sect. A: Accel. Spectrometers, Detect. Assoc. Equip.* **506**, 250–303, DOI: https://doi.org/10.1016/S0168-9002(03)01368-8 (2003).

81. Allison, J. *et al.* Geant4 developments and applications. *IEEE Transactions on Nucl. Sci.* **53**, 270–278, DOI: 10.1109/TNS.2006.869826 (2006).

82. Allison, J. *et al.* Recent developments in geant4. *Nucl. Instruments Methods Phys. Res. Sect. A: Accel. Spectrometers, Detect. Assoc. Equip.* **835**, 186–225, DOI: https://doi.org/10.1016/j.nima.2016.06.125 (2016).

83. https://datadiscovery.nlm.nih.gov/d/ux2j-9i9a.

Acknowledgements

Not applicable.

Funding

We acknowledge financial support from the "Tuscany Health Ecosystem (THE) Spoke 1, Advanced Radiotherapies and Diagnostics in Oncology" funded by the NextGenerationEU (PNRR), Codice progetto ECS00000017, D.D. MUR No. 1055 23 May 2022. We also acknowledge contributions from the following projects: NextGeneration EU Integrated Infrastructure Initiative in Photonic and Quantum Sciences (IPHOQS) CUP B53C22001750006, ID D2B8D520, IR0000016; Horizon 2020 Framework Programme Research and Innovation; Program EuPRAXIA Preparatory Phase (No. 101079773); EuPRAXIA Advanced Photon Sources—EuAPS (CUP I93C21000160006, IR0000030), INFN CSN5 funded project "FRIDA"; JRA ENI-CNR on Fusion energy (CUP B34I19003070007, CNR DFM.AD006.155); EU Horizon 2020 Research and Innovation Program EuPRAXIA Preparatory Phase (No. 101079773).

Author contributions statement

L.A.G., L.L. and D.D.S. conceived the study, L.A.G., L.L. and D.D.S. and D.P. conceptualised the MC modeling, F.A., L.L., D.D.S. and D.T. carried out the simulations, L.L., D.D.S. and L.A.G. analysed the results. S.P. and G.B. carried out dosimetric validation of the VHEE beam, L.A.G. coordinated the team. All authors reviewed the manuscript.

Competing interests

L.A.G., G.B. and L.L. are listed as inventors on an Italian industrial patent (application number: IT 102026000000715, granted by the Italian Patent and Trademark Office), which can potentially cover a technology related to the work described in this manuscript. The remaining authors declare no competing interests.

Supplementary Files

This is a list of supplementary files associated with this preprint. Click to download.

- SupplementaryMaterials.pdf